Study of Machining Characteristics of Non-conventional Methods

Rakesh R. Kolhapure[1,2](✉) and Duradundi S. Badkar[1,2]

[1] Shivaji University, Kolhapur, India
rockkolhapure@gmail.com
[2] Faculty of Engineering, YSPM's, Yashoda Technical Campus, Satara, India

Abstract. Smart alloy, which is typically called a shape memory alloy (SMA), have wide application in industry such as in aircraft, spacecraft, automotive, robotics, in civil structures, piping, medical field, engines, due to its shape memory effect, biocompatibility, strong resistance against corrosion, anti-fatigue characteristic. In a traditional machining method, physical contact occurs between workpiece and tool (SMA); therefore, increased tool wear and lesser dimensional stability due to pseudo-plasticity occur, which is not feasible. In contrast, different non-traditional machining methods are there, such as electrochemical machining (ECM), water jet machining (WJM), electro discharge machining (EDM), and wire electro-discharge machining (WEDM). The objective of this present work is to find a research gap. Based on the gap in a future new method, results get develop.

Keywords: Shape memory alloy · Wire electro-discharge machining · traditional machining · non-traditional machining

1 Introduction

Due to its unique qualities such as super elasticity, strong resistance against corrosion, high fatigue resistivity, and shape memory effects, Titanium-Nickel SMA has been used in biomedical and industrial engineering sectors [1]. The medical application includes optometry, orthopaedic surgery, dental, whereas industrial engineering includes engines, robotics, spacecraft [2] and in automotive safety industry [3]. SMAs are widely used in the civil field to reduce the effect caused by earthquakes or by environmental effects [4]. Different SMAs have been used in recent years, with Ti-Ni SMA being the most popular due to its higher damping capability, biocompatibility, corrosion resistance, and fatigue strength [5]. In Ti-Ni alloy Ti have a vindicatory layer (Ti O2), whereas Ni ions discharge into biofluid; as a result, this is the most widely used for biomedical implants [6]. Several researchers have described the effect of ternary alloying materials of SMAs. The addition of Co in Ti-Ni, with a decrease in Ni in Ti-Ni, leads to improved mechanical and physical properties, making it the most demanding material for biomedical application [7]. The addition of Cu content on Cu-based SMA increases martensitic temperature [8]. So, using SMAs as a material in several sectors, machining these alloys is essential.

S. Tamane et al. (Eds.): ICAMIDA 2022, ACSR 105, pp. 288–305, 2023.
https://doi.org/10.2991/978-94-6463-136-4_26

2 Traditional Machining of SMAs

Ti-Ni-based SMAs exhibit two properties: shape memory effect and superelasticity, they are quite popular in the medical field, in aerospace, precision machining with proper dimensional stability is significant with lower production cost. Good machinability is essential for a complex and intricate profile and accurate dimensions [9]. In the medical field (orthopaedic implants, orthodontic clips), surface finish plays a vital role. Moreover, obtaining such is a very challenging task in the manufacturing area. During the machining process, heat is generated at machining surface area which affects the performance of machinability [10]. Because of the existence of strain hardening effect, intermetallic compounds, cyclic hardening, and adhesion of alloy fragments to tool's surface, these characteristics of SMA lead to processing difficulties [8]. During the machining process, heat is generated; as a result, phase transformation taking place. So this phase transformation of SMAs made it very difficult to machine [11]. Do conventional machining is difficult due to its inaccurate dimensions, maximum tool wear rate as well as high-temperature generation during machining. Different non-conventional machining processes exist to avoid the challenges mentioned above caused by traditional machining procedures; other non-conventional machining processes are there. These non-conventional machining methods give better surface characteristics than conventional machining methods [12]. As a result, this research focuses on the work done by several non-conventional machining methods.

3 Non-traditional Machining of SMAs

To defeat challenges caused by conventional machining, some of the non-conventional methods, such as water jet machining [WJM], Electric discharge machining [EDM], electrochemical machining [ECM], and Wire electric discharge machining [WEDM].

3.1 Laser Machining

Under laser micro-cutting, the thermomechanical and metallurgical characteristics of a thick NiTiCu SMA sample were investigated. The findings reveal that thermal changes were observed on sample cut, and the fact that this exists is frequently used in the industry, which requires specific calorimetric qualities, in the industry, which needs particular calorimetric properties [13]. It was investigated how different input process parameters affected the laser's ability to create microchannels in NiTi SMAs as well as how those factors affected other properties. The result shows that the microchannel's quality is affected mainly by its input process parameters [14].

3.2 Electrochemical Machining

The effect of machining NiTi SMA with electrochemical micromachining utilizing a water-free electrolyte NaCl comprising ethylene glycol solution was investigated. A 20% volume amount of ethanol was supplementary to an ethylene glycol NaCl solution to improve machining superiority and surface roughness. It also reduces the formation of oxides films. While, excessive ethanol affects machining and surface quality [15]. The same results were noted on Titanium material [16]. Investigations were conducted to determine the effects of changing the power source and machining time during the SPECM process on the micro-grooves in Ni-Ti SMA [17].

3.3 Water Jet Machining

On Ni49.8Ti50.2 SMA, the effect of plain, as well as abrasive water jet machining, were examined. Experimental results suggest that the abrasive water jet approach is superior to the plain water jet method for milling depth control. It also discovered that abrasive water jet milling for milling NiTi SMA might be an effective and efficient method with a complicated crystal structure and phase change [18]. Researchers examined the outcome of procedure settings on geometrical precision and integrity using multi-mode abrasive water jet machining of NiTi SMAs. This study revealed better surface quality generated by controlling process parameters, which may machine a part in the aerospace industry [19].

3.4 EDM of SMAs

3.4.1 Material Removal Rate (MRR) in EDM

EDM characteristic, Ni60Al24.5Fe15.5 ternary SMA was investigated. Result states that MRR rises as discharge current rises. The maximum amount of material will be melted by a high discharge current's high current density. The melting point ratio (MRR) was calculated using the material's heat conductivity and melting temperature [20]. On NiTi SMA, the influence of EDM on the surface zone was investigated. In this, MRR is primarily determined by the electric discharge current between tool and workpiece. The material on the surface is removed by the melting and vaporization of the spark. MRR increases as discharge energy increases [21]. The effect of NiTi SMA micro-EDM was investigated. The effect of several input factors, such as capacitance, discharge voltage and different electrode material, on micro-hole quality was investigated. Results showed that MRR is greatly affected by capacitance. MRR increases with an increase in capacitance. As brass electrodes exhibit low thermal conductivity than tungsten electrodes, MRR is high for a brass electrode compared to a tungsten electrode [22]. In the EDM process for ternary SMA Ti35.5Ni48.5Zr16, MRR is increasing linearly with discharge current. It has found a reverse relationship between MRR and product of melting temperature and material thermal conductivity [23]. MRR is primarily dependent upon pulse duration. As a result of the increased pulse duration, the maximum amount of current flows and the MRR rises. Higher discharge current melt surface of workpiece very rapidly, therefore, MRR high [24].

3.4.2 Surface Integrity in EDM

Surface texture increases as the pulse current and intensity rises in EDM. When a higher pulse current is used to remove the most material, the surface quality suffers. Surface roughness increases as pulse energy increases [23, 24]. A comparative study was carried out of Nitinol SMA. The result shows that for laser machining to get an improvement in surface quality, minimum machining is required. As a result of the narrower markings formed on the surface, a good surface quality is attained [25]. Due to less discharge energy, less the surface gets melt result in a better surface finish. Due to high-discharge current, a more considerable amount of discharges hits the surface area of the workpiece, resulting in deterioration of surface being taking place, which affects surface quality. As the duration of the pulse lengthens, the discharge becomes greater and deeper. The roughness of the workpiece's surface tends to increase when it is depressed [20].

Figure 1 and Fig. 2 shows the material hardness of Ti35.5 Ni48.5Zr16, Ni60Al24.5Fe15.5, and Ni60Al24.5Fe55.5 ternary SMAs at different depths with respect to the machined surface. The workpiece has a high hardness nearer the machined surface and as distance increases, the hardness gets decreases, and at a certain level onward, it is almost the same as that of specimen hardens. This hardening arises because of different surface oxides forming Fe2O3, TiO, ZrO2, NiO, and Al2O3 in react layer [20, 23].

Figure 3a and Fig. 3b show that a recast layer on workpiece's machined surface during EDMing. As Ton rises, thickness of the recast layer is also continuously increases. Also observed in Fig. 3c and Fig. 3d. The increase in Ton increases the amount of electric energy that forms the recast layer on machined surface. An increase in electric energy makes more material be melted and resolidified. Therefore recast layer become larger [23]. Figure 4 shows the recast layer; melting drops and discharge craters are visible on machined surface. At greater Ton and peak currents, melting drops and bigger discharge craters are seen [20].

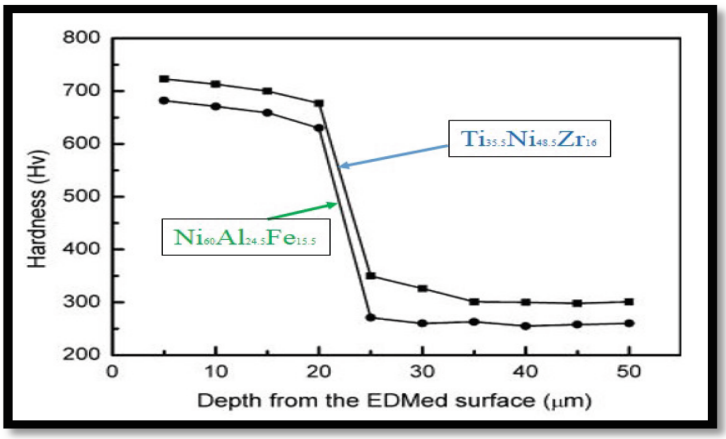

Fig. 1. EMDed Surface Hardness vs Depth [23]

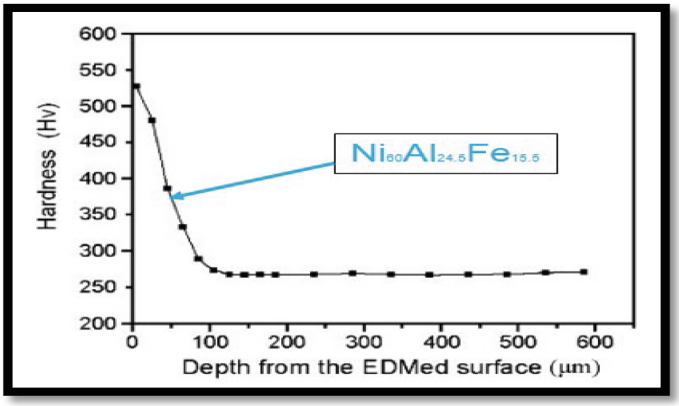

Fig. 2. EMDed Surface Hardness vs Depth [20]

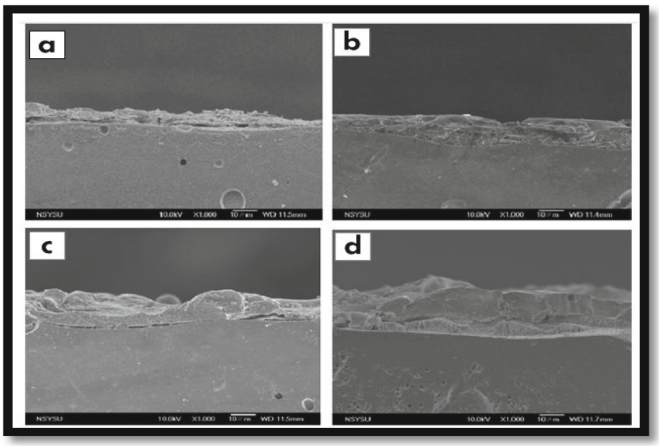

Fig. 3. Micrographs of $Ti_{35.5}Ni_{48.5}Zr_{16}$ for Discharge current = 7 A with (a) 3 μs, (b) 12 μs (c) 25 μs and (d) 50 μs Pulse duration [23]

3.5 WEDM of SMAs

3.5.1 MRR in WEDM

As more heat is produced at the spark gap, MRR rises in tandem with wire feed, resulting in more hot material splashing out and a greater MRR [26]. MRR rises when the pulse rate rises over time. The highest amount of energy is created because of the longer Ton, causing a high MRR [6]. Because the intensity of spark is very high at a high Ton, the highest thermal energy is available, and as a result, the maximum quantity of material from the material surface is eliminated. A longer Toff results, smaller MRR. This is because of a drop in spark intensity resulting from extra time for the dielectric fluid to flow, resulting in a low MRR [27]. With an increase in peak current, MRR rises. As peak current increases, spark and surface energy increase, leading to higher MRR [1].

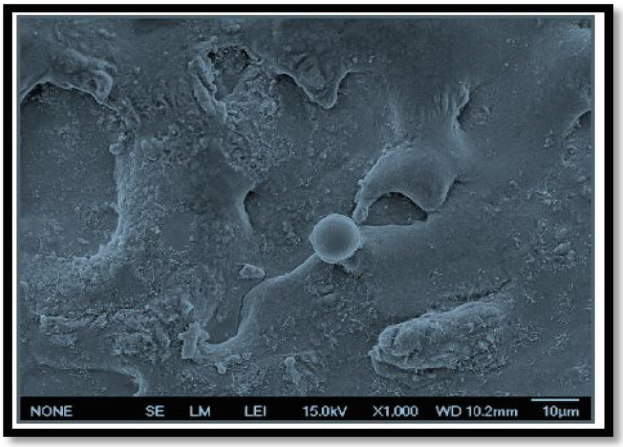

Fig. 4. SEM micrograph of EDM for the $Ni_{60}Al_{24.5}Fe15.5$ [20]

3.5.2 Surface Integrity in WEDM

Capacitance is strongly affected by surface roughness. Increase in capacitance results in high discharge energy with debris. It reduces surface quality. Hence lower surface roughness. Greater discharge energy causes larger crater formation results in larger surface roughness [28]. Surface roughness is mostly determined by cater size and energy discharged between electrode and workpiece. Roughness of surface rises as the Ton increases. More discharge energy occurs because of the longer pulse, resulting in a faster rate of crater formation, which rises surface roughness [29]. The rate of surface roughness decreases when the Toff is increased. Shorter ignition leads to tiny craters forming, and hence surface roughness reduces as the Toff rises. Increased peak current leads to increased maximum spark energy and crater size, as well as increased surface roughness [1]. The surface quality depends on dielectric fluid used during machining, wire material and flushing pressure [8]. Figure 5 shows micro-hardness on machined surface, an analysis was performed up to 100 μm deepness from the machined surface. As machining depth increases, the machined surface's microhardness gets reduced [30]. Three layers are formed during machining; the topmost layer is the recast layer, subsequently a heat-affected region and the converted zone layer beneath. From Fig. 6, it is clear that transformed layer region is not much affected by machining process results in converted layer hardness is almost the same as that of base material hardness [7].

Microglobules, recast deposits, melted droplets, fissures, blowholes, and craters on a machined surface are depicted in Fig. 7 and Fig. 8. Due to the high Ton, more thermal energy is produced, melting more material from the work piece's surface and causing craters and melting drops to form on the machined surface, resulting in a poor surface quality [7]. Due to the work piece's heating and cooling during the machining process, a recast layer develops close to the machined surface. The recast layer's thickness will increase with a longer Ton, but it can be decreased with a longer Toff. Less spark is produced and more time is spent cleaning away molten material as a result of the longer Toff [30].

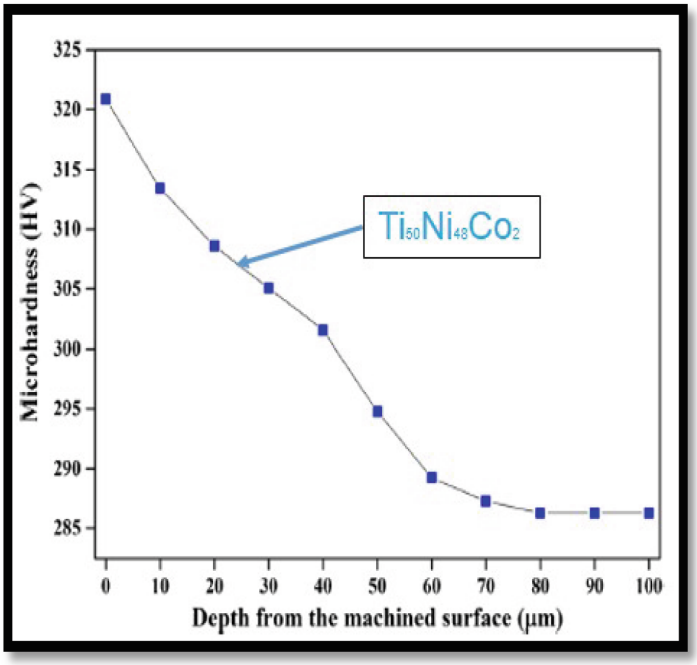

Fig. 5. WEMDed Surface Hardness vs. Depth [30]

Table 1 and Table 2 gives data of input parameters with their levels on machining of SMAs. It also gives different methods used for conducting experiments and also results. Different authors have selected different input parameters with different levels, and they studied its effects on mostly MRR, SR, and surface integrity. The Ton, Toff, servo voltage and current as a process parameter have been recorded in a few author's works. Wire feed, capacitance, electrode material, and dielectric fluid as a process parameter have been recorded in a few authors' publications. Few researchers used only Taguchi methods. Few researchers used the Taguchi method and some different optimization methods to study the impact of process variables of non-conventional machining on responses shown in Table 1 and Table 2. Other statistical tool techniques relate to input and output parameters such as Grey Relational Analysis, Response Surface Methodology, mixed orthogonal array, particle swarm optimization.

Table 3 gives the application of SMAs using non-conventional machining. Ni-Ti SMAs are frequently employed in biomedical research, aerospace. Due to good bio-compatibility with the excellent corrosion resistance of Ni-Ti SMA, widely used in medical applications.

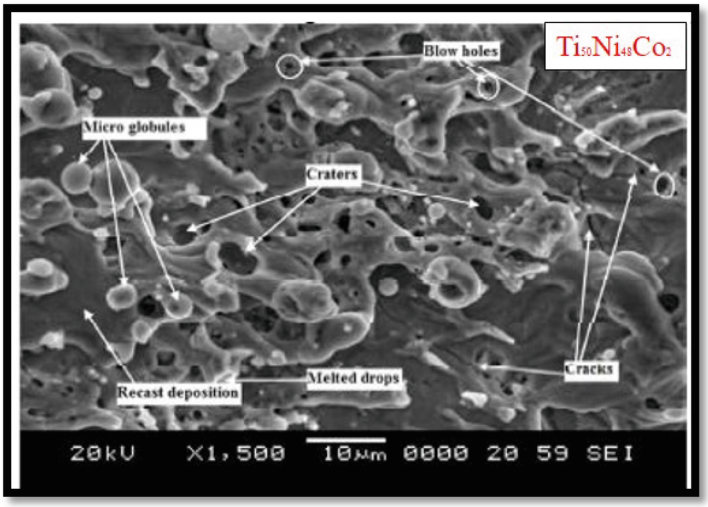

Fig. 8. SEM micrograph WEDMed surface [30]

Table 1. Study of nonconventional SMAs machining parameters for WEDM

Sr. No.	Authors	Input Variables	Material	Methods	Results	Values
1	[6]	Ton, T_{off} and Peak Current	$Ni_{54.1}Ti$ SMA	Taguchi Mixed L27 OA	1. The most significant parameter is the T_{on}. 2. As the T_{on} grows, the MRR and surface quality increase.	8–26 μs, 40–56 μs, 160–200 A
2	[31]	Wire Feed, Spark Voltage, T_{on}, T_{off}	$Ni_{55.8}Ti$ SMA	Taguchi L16 OA	1. Maximum MRR occurs when the voltage, T_{on}, and wire feed have risen. 2. The non-dominated sorting algorithm-II enhanced surface grade with process productivity at a single set.	20–50 V, 0.35–1 μs, 9–24 μs, 3–12 m/min

(*continued*)

Table 1. (*continued*)

Sr. No.	Authors	Input Variables	Material	Methods	Results	Values
3	[30]	T_{on}, T_{off}, Spark Voltage.	$Ti_{50}Ni_{48}Co_2$ SMA	Taguchi L9 OA	1. From optimum process parameters greater MRR, improved surface roughness, and a more robust machined surface were obtained. 2. During the microhardness study technique, micro fractures and microspheres were detected within the machined surface.	115–125 µs, 30–40 µs, 40–50 A
4	[27]	T_{on} and Spark Voltage	$Ti_{50}Ni_{49}Co_1$ SMA	Taguchi L25 method	1. Larger the T_{on}, higher will be cutting speed, which increases Spark Voltage result in a decrease in cutting speed. 2. At higher Spark Voltage, better SR was obtained. 3. Inverse relation were found between machined surface quality and cutting speed.	105–125 µs, 20–60 V
5	[11]	Servo voltage, T_{on}, T_{off}, current, wire speed.	Nickel-Titanium SMA	Taguchi L18 OA, Artificial neural network	1. The factor that has the greatest impact on MRR and SR is servo voltage. 2. Confirm that the test results are obtained by using GA are consistent with the experimental values.	20–50 V, 6–9 µs, 7–9 µs, 1–3 A, 0–2 m/min
6	[7]	T_{on}, T_{off} and servo voltage	$Ti_{50}Ni_{49}Co_5$ SMA	Taguchi L9 OA	1. Increase in T_{on} enhance MRR and Ra, whereas T_{off} and servo voltage lower them.	115–125 µs, 30–40 µs, 40–50 V

Table 2. Study of nonconventional SMAs machining parameters for EDM

Sr. No.	Authors	Input Variables	Material	Methods	Results	Values
1	[32]	T_{on}, T_{off}, Discharge Current and Duty cycle	Ni-Ti SMA	Taguchi L9 OA	1. The most influential process parameter on surface roughness is T_{off}. 2. Optimum surface roughness value is 4.25 μm.	50–150 μs, 50–80 μs, 2–8 A, 40–60%
2	[22]	Capacitance, Discharge voltage and Electrode material	Ni-Ti SMA	MOGA-II	1. The process variables that have the most effects on μEDM. Are capacitance and electrode material.	115–475 pF, 80–100 V, Brass and Tungsten
3	[33]	Capacitance, Discharge voltage, Electrode rotational speed, Dielectric and Electrode material	Ni-Ti SMA and Ti-6Al-4V	–	1. In comparison to Ti-6Al-4V, Ni-Ti SMA produces a finer surface quality.	1000 pF, 60 V, 3500 rpm, EDM Oil, Tungsten Carbide.

Table 3. Application of non-conventional SMAs

Sr. No.	Authors	Method	Material	Application
1	[13]	Laser Machining	NiTiCu	Industrial
2	[24]	Dry EDM	TiNi SMA	Biomedical
3	[33]	μEDM	NiTi SMA and Ti-6Al-4V	Orthopaedic and Orthodontic
4	[26]	WEDM	$Ti_{49.4}Ni_{50.6}$ SMA	Biomedical

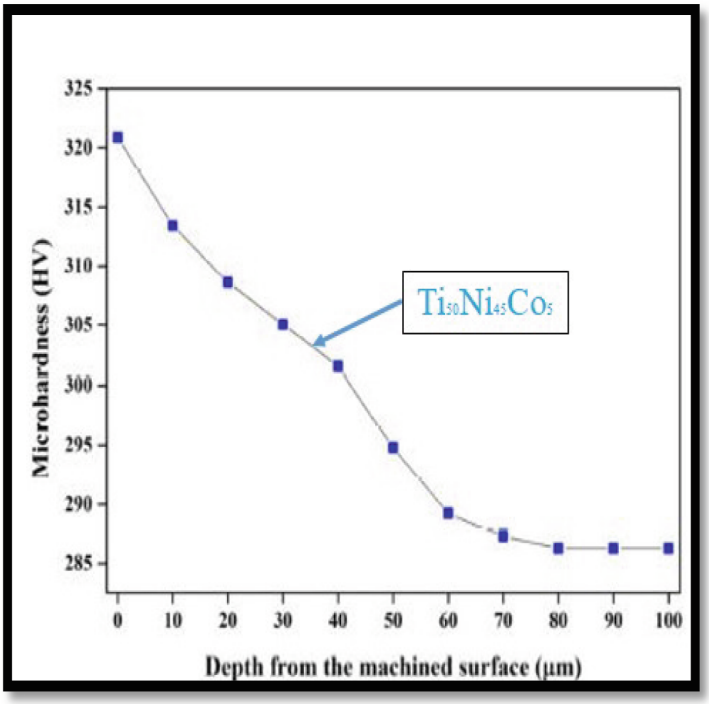

Fig. 6. WEMDed Surface Hardness vs. Depth [7]

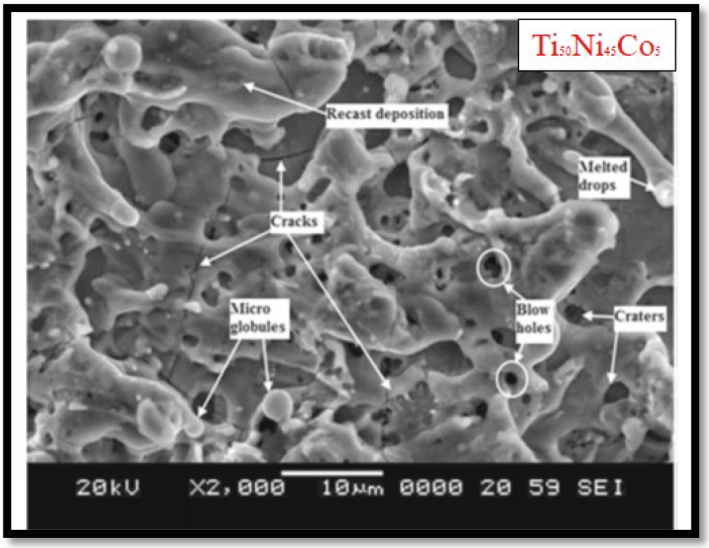

Fig. 7. Microstructure analysis of WEDMed surface [7]

Table 4. Investigational results comparison for tertiary elements

Sr. No.	Author	Material	Input Parameters									Output		
			Pulse on Time	Pulse off Time	Servo Voltage	Wire Feed	Wire Tension	Spark Gap Voltage	Current	Table Feed	Servo Speed	Material Removal Rate	Surface Roughness	Other
1	[30]	$Ni_{50}Ti_{48}Co_2$	√	√	√	–	–	–	–	–	–	√	√	–
2	[27]	$Ti_{50}Ni_{49}Co_1$	√	–	√	–	–	–	–	–	–	–	√	Cutting Speed
3	[34]	$Ti_{50}Ni_{40}Co_{10}$	√	√	√	√	–	–	–	–	√	√	√	–
4	[7]	$Ti_{50}Ni_{45}Co_5$	√	√	√	–	–	–	–	–	–	√	√	–
5	[2]	$Ti_{50}Ni_{45}Cu_5$	√	√	–	–	–	–	√	√	–	√	√	–

Table 5. Experimental results comparison for binary elements

Sr. No.	Authors	Material	Input Parameters									Output		
			Pulse on Time	Pulse off Time	Servo Voltage	Wire Feed	Wire Tension	Spark Gap Voltage	Current	Input Power	Flushing Pressure	Material Removal Rate	Surface Roughness	Other
1	[5]	$Ni_{50.6}Ti_{49.4}$	√	√	√	√	– –	–	–	√	–	√	√	–
2	[35]	$Ni_{49}Ti_{51}$	√	√	–	√	√	–	–	–	–	√	√	–
3	[36]	$TiNi_{55.78}$	√	√	–	–	–	–	√	–	–	√	√	–
4	[6]	$Ni_{54.1}Ti$	√	√	–	–	–	–	√	–	–	√	√	–
5	[26]	$Ni_{50.6}Ti_{49.4}$	√	√	√	√	√	–	–	–	–	√	√	–
6	[1]	$TiNi_{55.7}$	√	√	–	–	–	–	√	–	–	√	√	–
7	[37]	Nitinol	√	–	–	√	–	–	√	–	√	–	√	–
8	[38]	$Ni_{54.89}Ti_{44.84}$	√	–	–	√	√	–	√	–	√	–	√	–
9	[39]	$Ti_{44.13}$ $Ni_{55.74}$	√	√	–	–	–	√	–	–	–	√	√	–
10	[42]	$TiNi_{55.8}$	√	√	–	–	–	–	√	–	–	√	√	–
11	[43]	Nitinol	√	√	√	–	–	–	√	–		√	√	–
12	[40]	Ti_{60} Ni_{40}	√	√	–	–	√	–	√	–	--	–	√	Cutting Rate, Dimensional Shift
13	[41]	Ti $Ni_{55.8}$	√	√	–	–	–	–	√	–	–	√	√	Microhardness

√: Considered by authors; –: Not considered by authors

Table 6. Output values for different materials

Authors	Material	Material Notation	MRR	SR
[5]	$Ni_{50.6}Ti_{49.4}$	A	9.655	2.664
[36]	Ti $Ni_{55.78}$	B	0.5262	1.27
[6]	$Ni_{54.1}$Ti	C	5.502	1.489
[26]	$Ni_{50.6}Ti_{49.4}$	D	2.537	1.296
[39]	$Ti_{44.13}$ $Ni_{55.74}$	E	2.65	2.0188
[42]	Ti $Ni_{55.8}$	G	0.7259	7.189
[44]	Nitinol	H	1.9503	1.28
[41]	Ti $Ni_{55.8}$	I	1.1763	4.425
[43]	Nitinol	J	3.959	1.785

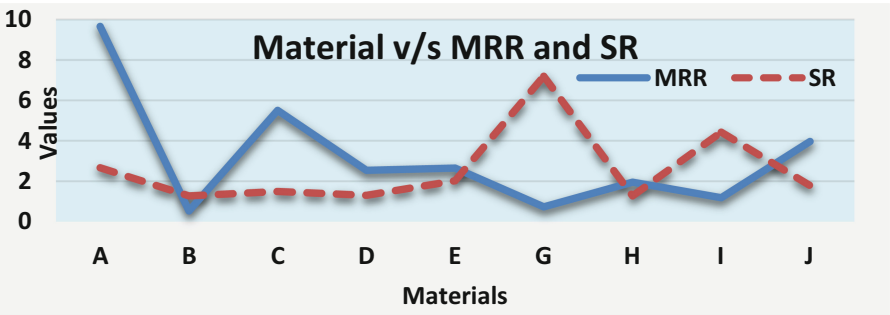

Graph 1. Material v/s MRR and SR

4 Discussion and Findings

After evaluating the literature survey for different materials for WEDM, the various findings related to input and output parameters are shown in Table 4, Table 5, and Table 6, along with Graph 1, shows the graphical analysis between different materials v/s Surface Roughness and Material Removal Rate.

Graph 1 and Table 6 represents MRR are SR inversely proportional. Better quality of surface is obtained at lower MRR.

5 Conclusion

Based on the reference presented in this paper for machining of Ni-Ti SMAs on EDM and WEDM following conclusions are drawn,

1. Good work has been carried out by considering T_{on}, T_{off}, servo voltage, spark current as a process parameter and their effect on responses.

2. However, there are few parameters on which study must be carried out: wire feed, wire tension, wire material, and dielectric fluid.
3. Micro hardness, surface roughness, microstructure, and elemental analysis are all process characteristics that must be investigated.

References

1. H. Bisaria and P. Shandilya, "Study on Effect of Machining Parameters on Performance Characteristics of Ni-rich NiTi Shape Memory Alloy during Wire Electric Discharge Machining," *Mater. Today Proc.*, vol. 5, no. 2, pp. 3316–3324,(2018), https://doi.org/10.1016/j.matpr.2017.11.574.
2. M. Manjaiah, S. Narendranath, S. Basavarajappa, and V. N. Gaitonde, "Wire electric discharge machining characteristics of titanium nickel shape memory alloy," *Trans. Nonferrous Met. Soc. China (English Ed.*, vol. 24, no. 10, pp. 3201–3209,(2014), https://doi.org/10.1016/S1003-6326(14)63461-0.
3. V.Gheorghita, P. Gümpel, A. Chiru, and A. J. Strittmatter, "Future Applications of Ni-Ti Alloys in Automotive," *Int. J. Automot. Technol.*, vol. 15, no. 3, pp. 469–474,(2014), 0.1007/s12239−014−0049−z.
4. G. Song, N. Ma, and H. N. Li, "Applications of shape memory alloys in civil structures," *Eng. Struct.*, vol. 28, no. 9, pp. 1266–1274, (2006), https://doi.org/10.1016/j.engstruct.2005.12.010.
5. J. Kesavan, C. Velmurugan, V. Senthilkumar, and S. Dinesh, "Optimization of WEDM parameters on surface integrity characteristics of NiTi shape memory alloy," *Mater. Today Proc.*, vol. 43, no. xxxx, pp. 183–190, (2020), https://doi.org/10.1016/j.matpr.2020.11.616.
6. D. K. Gupta and A. K. Dubey, "Multi process parameters optimization of Wire-EDM on shape memory alloy (Ni54.1Ti) using Taguchi approach," *Mater. Today Proc.*, vol. 44, no. xxxx, pp. 1423–1427,(2021), https://doi.org/10.1016/j.matpr.2020.11.628.
7. H. Soni, N. S. Narendranath, and M. Ramesh, "Experimental Investigation on Effects of Wire Electro Discharge Machining of Ti50Ni45Co5 Shape Memory Alloys," *Silicon*, vol. 10, no. 6, pp. 2483–2490,(2018), https://doi.org/10.1007/s12633-018-9780-9.
8. M. Manjaiah, S. Narendranath, and S. Basavarajappa, "Review on non-conventional machining of shape memory alloys," *Trans. Nonferrous Met. Soc. China (English Ed.*, vol. 24, no. 1, pp. 12–21, (2014) , https://doi.org/10.1016/S1003-6326(14)63022-3.
9. A. Khan, K. Academy, W. Jappes, K. Academy, S. R. Kumar, and J. Mashinini, "Machinability Of Shape Memory Alloy Using Electro Spark Erosion Process," pp. 1–13.
10. B. Dash, M. Das, M. Das, T. R. Mahapatra, and D. Mishra, "A concise review on machinability of niti shape memory alloys," *Mater. Today Proc.*, vol. 18, pp. 5141–5150, (2019) https://doi.org/10.1016/j.matpr.2019.07.511.
11. C. Velmurugan, V. Senthilkumar, S. Dinesh, and D. Arul Kirubakaran, "Artificial neural network prediction of wire electrical discharge machining properties on sintered porous NiTi shape memory alloy," *Mater. Today Proc.*, vol. 5, no. 2, pp. 8382–8390, (2018), https://doi.org/10.1016/j.matpr.2017.11.532.
12. C. Velmurugan, V. Senthilkumar, S. Dinesh, and D. Arulkirubakaran, "Machining of NiTi-shape memory alloys-A review," *Mach. Sci. Technol.*, vol. 22, no. 3, pp. 355–401, (2018), https://doi.org/10.1080/10910344.2017.1365894.
13. C. A. Biffi *et al.*, "Effect of laser microcutting on thermo-mechanical properties of NiTiCu shape memory alloy," *Met. Mater. Int.*, vol. 20, no. 1, pp. 83–92, (2014), https://doi.org/10.1007/s12540-013-6011-1

14. M. K. Mohammed and A. Al-Ahmari, "Laser-machining of microchannels in NiTi-based shape-memory alloys: Experimental analysis and process optimization," *Materials (Basel).*, vol. 13, no. 13, (2020), https://doi.org/10.3390/ma13132945.
15. S. Ao *et al.*, "Electrochemical micromachining of NiTi shape memory alloy with ethylene glycol–NaCl electrolyte containing ethanol," *J. Manuf. Process.*, vol. 53, no. February, pp. 223–228, (2020), https://doi.org/10.1016/j.jmapro.2020.02.019.
16. W. Liu *et al.*, "Electrochemical micromachining on titanium using the NaCl-containing ethylene glycol electrolyte," *J. Mater. Process. Technol.*, vol. 255, pp. 784–794, (2018), https://doi.org/10.1016/j.jmatprotec.2018.01.009.
17. E. S. Lee, T. H. Shin, B. K. Kim, and S. Y. Baek, "Investigation of short pulse electrochemical machining for groove process on Ni-Ti shape memory alloy," *Int. J. Precis. Eng. Manuf.*, vol. 11, no. 1, pp. 113–118, (2010), https://doi.org/10.1007/s12541-010-0014-3.
18. M. C. Kong, D. Axinte, and W. Voice, "Challenges in using waterjet machining of NiTi shape memory alloys: An analysis of controlled-depth milling," *J. Mater. Process. Technol.*, vol. 211, no. 6, pp. 959–971, (2011), https://doi.org/10.1016/j.jmatprotec.2010.12.015.
19. M. C. Kong, D. Srinivasu, D. Axinte, W. Voice, J. McGourlay, and B. Hon, "On geometrical accuracy and integrity of surfaces in multi-mode abrasive waterjet machining of NiTi shape memory alloys," *CIRP Ann. - Manuf. Technol.*, vol. 62, no. 1, pp. 555–558,(2013), https://doi.org/10.1016/j.cirp.2013.03.021.
20. S. L. Chen, S. F. Hsieh, H. C. Lin, M. H. Lin, and J. S. Huang, "Electrical discharge machining of a NiAlFe ternary shape memory alloy," *J. Alloys Compd.*, vol. 464, no. 1–2, pp. 446–451, (2008), https://doi.org/10.1016/j.jallcom.2007.10.012.
21. W. Theisen and A. Schuermann, "Electro discharge machining of nickel-titanium shape memory alloys," *Mater. Sci. Eng. A*, vol. 378, no. 1–2 SPEC. ISS., pp. 200–204, (2004), https://doi.org/10.1016/j.msea.2003.09.115.
22. M. H. Abidi, A. M. Al-Ahmari, U. Umer, and M. S. Rasheed, "Multi-objective optimization of micro-electrical discharge machining of nickel-titanium-based shape memory alloy using MOGA-II," *Meas. J. Int. Meas. Confed.*, vol. 125, no. February 2017, pp. 336–349, (2018), https://doi.org/10.1016/j.measurement.2018.04.096.
23. S. F. Hsieh, A. W. J. Hsue, S. L. Chen, M. H. Lin, K. L. Ou, and P. L. Mao, "EDM surface characteristics and shape recovery ability of Ti 35.5Ni48.5Zr16 and Ni60Al 24.5Fe15.5 ternary shape memory alloys," *J. Alloys Compd.*, vol. 571, pp. 63–68, (2013), https://doi.org/10.1016/j.jallcom.2013.03.111.
24. T. S. Huang, S. F. Hsieh, S. L. Chen, M. H. Lin, S. F. Ou, and W. T. Chang, "Surface modification of TiNi-based shape memory alloys by dry electrical discharge machining," *J. Mater. Process. Technol.*, vol. 221, pp. 279–284,(2015), https://doi.org/10.1016/j.jmatprotec.2015.02.025.
25. C. H. Fu, J. F. Liu, Y. B. Guo, and Q. Z. Zhao, "A Comparative Study on White Layer Properties by Laser Cutting vs. Electrical Discharge Machining of Nitinol Shape Memory Alloy," *Procedia CIRP*, vol. 42, no. Isem Xviii, pp. 246–251, (2016), https://doi.org/10.1016/j.procir.2016.02.280.
26. A. M. Takale and N. K. Chougule, "Effect of wire electro discharge machining process parameters on surface integrity of Ti49.4Ni50.6 shape memory alloy for orthopedic implant application," *Mater. Sci. Eng. C*, vol. 97, no. November 2018, pp. 264–274, (2019), https://doi.org/10.1016/j.msec.2018.12.029.
27. H. Soni, S. Narendranath, and M. R. Ramesh, "Effects of Wire Electro-Discharge Machining Process Parameters on the Machined Surface of Ti 50 Ni 49 Co 1 Shape Memory Alloy," *Silicon*, vol. 11, no. 2, pp. 733–739, (2019), https://doi.org/10.1007/s12633-017-9687-x.
28. B. Kuriachen, K. P. Somashekhar, and J. Mathew, "Multiresponse optimization of micro-wire electrical discharge machining process," *Int. J. Adv. Manuf. Technol.*, vol. 76, no. 1–4, pp. 91–104, (2015), https://doi.org/10.1007/s00170-014-6005-2.

29. M. Manjaiah, S. Narendranath, and S. Basavarajappa, "Wire Electro Discharge Machining Performance of TiNiCu Shape Memory Alloy," *Silicon*, vol. 8, no. 3, pp. 467–475, (2016), https://doi.org/10.1007/s12633-014-9273-4.
30. D. Reddy, H. Soni, and S. Narendranath, "Experimental investigation and optimization of WEDM process parameters for Ti50Ni48Co2 shape memory alloy," *Mater. Today Proc.*, vol. 5, no. 9, pp. 19063–19072, (2018), https://doi.org/10.1016/j.matpr.2018.06.259.
31. R. Magabe, N. Sharma, K. Gupta, and J. Paulo Davim, "Modeling and optimization of Wire-EDM parameters for machining of Ni55.8Ti shape memory alloy using hybrid approach of Taguchi and NSGA-II," *Int. J. Adv. Manuf. Technol.*, vol. 102, no. 5–8, pp. 1703–1717, (2019), https://doi.org/10.1007/s00170-019-03287-z.
32. A. Gangele and A. Mishra, "Surface roughness optimization during machining of NiTi shape memory alloy by EDM through Taguchi's technique," *Mater. Today Proc.*, vol. 29, pp. 343–347, (2018), https://doi.org/10.1016/j.matpr.2020.07.287.
33. M. P. Jahan, P. Kakavand, and F. Alavi, "A Comparative Study on Micro-electro-discharge-machined Surface Characteristics of Ni-Ti and Ti-6Al-4V with Respect to Biocompatibility," *Procedia Manuf.*, vol. 10, pp. 232–242,(2017), https://doi.org/10.1016/j.promfg.2017.07.051.
34. H. Soni, N. Sannayellappa, and R. M. Rangarasaiah, "An experimental study of influence of wire electro discharge machining parameters on surface integrity of TiNiCo shape memory alloy," *J. Mater. Res.*, vol. 32, no. 16, pp. 3100–3108,(2017), https://doi.org/10.1557/jmr.2017.137.
35. A. Goyal, H. UR Rahman, and S. A. C. Ghani, "Experimental investigation & optimisation of wire electrical discharge machining process parameters for Ni49Ti51 shape memory alloy," *J. King Saud Univ. - Eng. Sci.*, vol. 33, no. 2, pp. 129–135,(2021), https://doi.org/10.1016/j.jksues.2020.01.003.
36. R. Chaudhari *et al.*, "Experimental investigations and optimization of MWCNTs-mixed WEDM process parameters of nitinol shape memory alloy," *J. Mater. Res. Technol.*, vol. 15, pp. 2152–2169, (2021), https://doi.org/10.1016/j.jmrt.2021.09.038.
37. P. P. Das and S. Chakraborty, "A grey correlation-based TOPSIS approach for optimization of surface roughness and micro hardness of Nitinol during WEDM operation," *Mater. Today Proc.*, vol. 28, no. xxxx, pp. 568–573, (2019), https://doi.org/10.1016/j.matpr.2019.12.220.
38. H. Majumder and K. Maity, "Application of GRNN and multivariate hybrid approach to predict and optimize WEDM responses for Ni-Ti shape memory alloy," *Appl. Soft Comput. J.*, vol. 70, pp. 665–679, (2018), https://doi.org/10.1016/j.asoc.2018.06.026.
39. V. N. Kulkarni, V. N. Gaitonde, V. Hadimani, and V. Aiholi, "Analysis of Wire EDM process parameters in machining of NiTi superelastic alloy," *Mater. Today Proc.*, vol. 5, no. 9, pp. 19303–19312, (2018), https://doi.org/10.1016/j.matpr.2018.06.289.
40. N. Sharma, T. Raj, and K. K. Jangra, "Parameter optimization and experimental study on wire electrical discharge machining of porous Ni40Ti60 alloy," *Proc. Inst. Mech. Eng. Part B J. Eng. Manuf.*, vol. 231, no. 6, pp. 956–970,(2017), https://doi.org/10.1177/0954405415577710.
41. R. Chaudhari, J. J. Vora, S. S. M. Prabu, I. A. Palani, V. K. Patel, and D. M. Parikh, "Pareto optimization of WEDM process parameters for machining a NiTi shape memory alloy using a combined approach of RSM and heat transfer search algorithm," *Adv. Manuf.*, vol. 9, no. 1, pp. 64–80, (2021), https://doi.org/10.1007/s40436-019-00267-0.
42. P. Rathi, R. Ghiya, H. Shah, P. Srivastava, S. Patel,R. Chaudhari and J. Vora, "Multi-response Optimization of Ni55.8Ti Shape Memory Alloy Using Taguchi–Grey Relational Analysis Approach",pp.13-23, (2020), https://doi.org/10.1007/978-981-32-9971-9_2.
43. N. Chakala, P. S. Chandrabose, and C. S. P. Rao, "Optimisation of WEDM parameters on Nitinol alloy using RSM and desirability approach," *Aust. J. Mech. Eng.*, pp. 1–13, (2019), https://doi.org/10.1080/14484846.2019.1681239.

44. R. Chaudhari , J. Vora , S. S. Mani Prabu, I. A. Palani, V.K. Patel, D. M. Parikh and L. N. L. de Lacalle, "Multi-Response Optimization of WEDM Process Parameters for Machining of Superelastic Nitinol Shape-Memory Alloy Using a Heat-Transfer Search Algorithm," (2019), https://doi.org/10.3390/ma12081277.